Atmospheric Environment 248 (2021) 118229

Contents lists available at ScienceDirect

Atmospheric Environment

journal homepage: http://www.elsevier.com/locate/atmosenv

Physical and chemical characterization of the 2019 "black rain" event in the Metropolitan Area of São Paulo, Brazil

Guilherme Martins Pereira [a,b,*], Sofia Ellen da Silva Caumo [a], Adriana Grandis [c], Emerson Queiroz Mota do Nascimento [a], Alexandre Lima Correia [d], Henrique de Melo Jorge Barbosa [d], Marta Angela Marcondes [e], Marcos Silveira Buckeridge [c], Pérola de Castro Vasconcellos [a]

[a] Department of Chemistry, Institute of Chemistry, University of São Paulo, 05508-000, São Paulo, Brazil
[b] Department of Atmospheric Sciences, Institute of Astronomy, Geophysics and Atmospheric Sciences, University of São Paulo, 05508-090, São Paulo, Brazil
[c] Department of Botany, Institute of Biosciences, University of São Paulo, 05508-090, São Paulo, Brazil
[d] Department of Applied Physics, Institute of Physics, University of São Paulo, 05508-090, São Paulo, Brazil
[e] University of São Caetano do Sul, São Caetano do Sul, Brazil

HIGHLIGHTS

- Darkened precipitation was associated with smoke transport in São Paulo, Brazil.
- Intense fire episodes were observed in the Amazon deforestation arch and Bolivia.
- Satellite images and back trajectories revealed biomass burning aerosols transport.
- Monosaccharides and retene in the rain samples confirmed biomass burning influence.

GRAPHICAL ABSTRACT

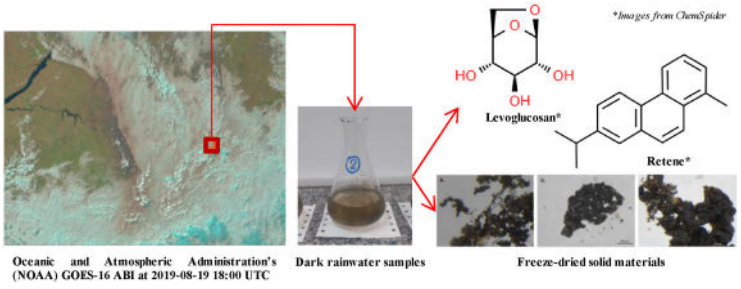

ARTICLE INFO

Keywords:
Rainwater
Biomass burning
Amazon
Monosaccharides
Polycyclic aromatic hydrocarbons

ABSTRACT

Aerosols emitted from biomass burning in South American tropical forests have been a concern in the last decades. On August 19th, 2019 darkened precipitation was observed over the metropolitan area of São Paulo (MASP), in an unprecedented event termed "black rain", after intense biomass burning episodes in the South American hinterland. Satellite imagery, back trajectory analyses, and meteorological reports showed air masses transporting thick plumes of biomass burning aerosols originated in part from the Amazon Basin and Bolivia. Rainwater samples were collected in different sites of the metropolitan area, during and after the "black rain" event, and both physically and chemically characterized to assess the possible influence of biomass burning aerosols in the event. The collected samples in the "black rain" event presented high turbidity (above 70 NTU), and biomass burning organic tracers (levoglucosan, mannosan, and galactosan) were observed in higher concentrations in the "black rain" samples than in control ones (e.g. average levoglucosan of 0.33 μg mL^{-1}, compared to 0.02 μg mL^{-1} after the event), with deposition fluxes more than three times higher during the event (1.04 mg m^{-2} and 0.31 mg m^{-2}, respectively). The detection of glucose, xylose, and mannose, after hydrolysis of the solid material present in the "black rain" samples, strongly suggested the presence of plant cell wall material

* Corresponding author. Department of Chemistry, Institute of Chemistry, University of São Paulo, 05508-000, São Paulo, Brazil.
E-mail address: guilherme.martins.pereira@usp.br (G.M. Pereira).

https://doi.org/10.1016/j.atmosenv.2021.118229
Received 13 August 2020; Received in revised form 1 January 2021; Accepted 20 January 2021
Available online 26 January 2021

derived from the partial combustion of wood and grass matter. Total polycyclic aromatic hydrocarbons (PAHs) concentrations were, in general, higher during the event than in post-event control samples collected in the MASP (on average, almost 15 times higher than after the event), with a higher deposition flux (5.1 and 2.7 mg m^{-2}, respectively). Overall, there are strong pieces of evidence that the long-range transport of smoke produced in South American forest fires was connected to the precipitation of darkened rainwater over the Metropolitan Area of São Paulo.

1. Introduction

Particulate matter (PM) emitted from biomass burning in Brazilian forests has attracted attention in the last decades. The emission of PM can influence the radiation balance and act as cloud condensation nuclei (CCN), modifying cloud properties (Andreae et al., 2004; de Oliveira Alves et al, 2014, 2015; Koren et al., 2004; Schkolnik et al., 2005; Sena et al., 2013). Precipitation acts as a sink, carrying out of the troposphere dissolved airborne organic carbon and ionic species, which can be emitted by both anthropogenic and natural sources (Altieri et al., 2008; Avery et al., 2006; Mead et al., 2013; Mullaugh et al., 2014; Vieira-Filho et al., 2013).

Most biomass burning emissions happen in tropical areas during dry periods and can be a dominant source of particulate matter, an essential climatic driver (Seinfeld and Pandis, 2006). In the Brazilian dry season, there is an increase in the emission of aerosols from biomass burning in the *Cerrado* (savanna) and the Amazon regions (de Oliveira Alves et al., 2015; Santos, 2014). Efforts have been made to ban sugarcane burning in the State of São Paulo and other places in the Central-South region of Brazil in the last decade and they were much reduced by 2017 (Andrade et al., 2017; de Almeida Silva et al., 2020; Pereira et al., 2019). The Amazon represents approximately half of the remaining tropical forests on the planet, corresponding to 62% of Brazilian territory (Malhi et al., 2008). Most of the forest fires in the Brazilian Amazon are located in an area of approximately 500,000 km^2, known as the deforestation arc, and are associated with land-clearing practices to give place to pastures and crops (Artaxo et al., 2013; de Oliveira Alves et al., 2015).

Previous studies have found that the emissions from biomass burning in the Amazon dry season may cause adverse effects to human health of the local exposed population; the particulate matter was observed to be both mutagenic and carcinogenic, with the potential risk of DNA damage, mutation, and cancer (de Oliveira Alves et al., 2014; de Oliveira Galvão et al., 2018). However, these biomass burning aerosols are lifted from the boundary layer into the free troposphere by clouds and pyro-cumulus clouds (Andreae et al., 2004; Darbyshire et al., 2019), from where they can be transported by winds for thousands of kilometers. Given the spatial scale of this transport, satellites are the most useful monitoring tool in South America (Edwards et al., 2006) and elsewhere (Duncan et al., 2003; Zhu et al., 2016). As a consequence of the long-range transport, these biomass burning aerosols can also affect the air quality in remote urban sites (Pereira et al., 2017a, 2017b; Vasconcellos et al., 2011).

Polycyclic aromatic hydrocarbons (PAHs) are important particulate organic compounds mainly emitted by anthropogenic sources (among them, biomass burning), and are frequently studied due to their carcinogenic properties (Pereira et al., 2017b; Ravindra et al., 2008). Because the burning of biomass is often incomplete, polysaccharides derived from plant biomass (e.g. cell wall components such as cellulose, xylans, and mannans) can be found in the particulate matter. The detection of such polymers can be done by measuring the levels of monosaccharides in atmospheric samples after the hydrolysis procedure. These findings can bring information about the transport of biological material and biomass burning aerosols emitted from remote places (Fu et al., 2012; Simoneit et al., 2004). The presence of sugar polymers in the biomass

Sample Label	Date	Site	Sample type
EZ	19th August	East Zone – São Paulo	Rain event
SZ	19th August	South Zone – São Paulo	Rain event
DI	19th August	Diadema	Rain event
SA	19th August	Santo André	Rain event
NZ	1st September	North Zone – São Paulo	Control
WZ1	1st September	West Zone – São Paulo	Control
WZ2	3rd September	West Zone 2 – São Paulo	Control
WZ2	5th September	West Zone 2 – São Paulo	Control
WZ2	6th September	West Zone 2 – São Paulo	Control

Fig. 1. Sampling site locations and dates.

burning related aerosol increases its hygroscopicity, and influences cloud albedo and cloud formation, possibly affecting climate (Mullaugh et al., 2014; Russell et al., 2009).

Particulate matter can be transported by air masses and taken to the surface by raindrops and other forms of precipitation by the so-called rain-out and wash-out processes (Cousins et al., 1999; Seinfeld, 2004). On August 19th, 2019, a unique phenomenon occurred over a significant extension of São Paulo State, Brazil, due to the convergence of a precipitating system and the transport of biomass burning aerosols. Smoke plumes originated from burning areas in both Brazilian and Bolivian Amazon Basin, and also from other parts of Bolivia, were captured by the South Atlantic Convergence Zone and brought over large cities in the Brazilian Southeast. A cold front induced moist marine air convergence, promoting cloud formation at lower and higher altitudes. An abnormal darkening of the sky and clouds was observed over the Metropolitan Area of São Paulo (MASP, −23.5505°, −46.6339°, 760 m above sea level), the most densely populated urban area in South America. Rainwater samples were collected during precipitation events. The samples presented an exceptionally darkened appearance and a characteristic odor of smoke. This event was referred to as the "black rain".

The objectives of this study are: (i) the physical (turbidity and microscopy) and chemical characterization (water-soluble ions, monosaccharides, and PAHs) of "black rain" water samples collected over the MASP after an intense biomass burning episode in several areas of South America hinterland, (ii) to analyze satellite imagery and air mass back trajectories, and (iii) to investigate the influence of biomass burning transported aerosols on the precipitation.

2. Materials and methods

Four samples were collected during the "black rain" precipitation event on August 19th, 2019, in sites around the MASP: eastern and southern zones of São Paulo (EZ and SZ), Diadema (DI), and Santo André (SA) (Fig. 1). The samples were collected in clean plastic bottles and since the event was unexpected these were the only samples available; those were the few sites with a significant accumulation of precipitation on that day. In the next days after the event, five control samples were collected in different sites. Two control samples were taken in the northern and western zones of São Paulo (NZ and WZ1) on September 1st, 2019. Three other control samples were collected on the rooftop of the Institute of Chemistry building, at the University of São Paulo main campus (WZ2), in a large glass beaker cleaned with ultrapure water, on September 3rd, 5th, and 6th. Thymol ($C_{10}H_{14}O$) was added to all samples as a biocide, and they were kept at −18 °C until analysis. After defrosting, the samples were quickly transferred to glassware for analytical further procedures.

The "black rain" samples collected in three sites (DI, EZ, and SA) were freeze-dried to concentrate particulate matter for microscopic imaging. The images were obtained using a stereomicroscope Leica M205 FA, lens 1. The pictures were processed in the Leica Application Suite software (LAS-version 4.8).

Water-soluble ions were determined in duplicate; Na^+, K^+, Ca^{2+}, Mg^{2+}, Cl^-, SO_4^{2-}, formate (CHO_2^-), oxalate ($C_2O_4^{2-}$), acetate ($C_2H_3O_2^-$), fumarate ($C_4H_2O_4^{2-}$), and glutarate ($C_5H_6O_4^{2-}$). The samples were analyzed after filtration (Millipore Millex, 0.22 μm), with an ion chromatograph (Metrohm, Switzerland), the same equipment employed by Vasconcellos et al. (2010). For monosaccharide anhydrides (levoglucosan, mannosan, and galactosan), 25 mL aliquots of the samples were frozen in glass amber flasks with dry ice in an ethanol bath (−72 °C), and lyophilized for two days, similarly as described by Mullaugh et al. (2014). After the lyophilization, the particulate residue was extracted with a mixture containing 80% of dichloromethane and 20% of methanol (40 mL) for 1 h in an ultrasonic bath, then dried up with a rotary evaporator and derivatized with 40 μL of a mixture of N-methyl--N-(trimethylsilyl)trifluoroacetamide (MSTFA) and pyridine (2:1; v/v) for 1 h, at 70 °C. After derivatization, the samples were analyzed in a gas chromatograph with a mass spectrometer detector (GC/MS). The extraction procedure of the particulate material was similar to that described in Pashynska et al. (2002). The recovery test was performed with the spiking of blank samples and the obtained values were 71, 91, and 94%, for levoglucosan, mannosan, and galactosan.

For PAHs, a sample aliquot of 10 mL was inserted in a glass separatory funnel (pH between 6 and 10), then 100 mL of dichloromethane was added, and then the funnel was vigorously shaken for 1 min, the procedure was repeated once more. The 200 mL extract was dried up with rotary evaporation, and then the extracts were analyzed in a GC/MS (EMS Parameter, 2017).

The method accuracy was evaluated in two ways: by using certified reference material and performing recovery tests. The PAHs mixture was prepared with standard which contained the following compounds: fluorene (FLU), phenanthrene (PHE), anthracene (ANT), fluoranthene (FLT), pyrene (PYR), benzo[*a*]anthracene (BaA), chrysene (CHR), benzo[*b*]fluoranthene (BbF), benzo[*k*]fluoranthene (BkF), benzo[*a*]pyrene (BaP), indeno[1,2,3-*cd*]pyrene (InP), dibenzo[*a,h*]anthracene (DBA) and benzo[*ghi*]perylene (BPer) (610 mix, Supelco, USA), benzo[*e*]pyrene (BeP) (Supelco, USA) and coronene (COR) (Sigma-Aldrich, USA). All the samples were analyzed in triplicate, and the three samples collected at the university campus (WZ2) were pooled before extraction since the concentrations of PAHs were below the detection limit in those samples.

For the recovery test, three aliquots of standard solution were extracted and analyzed under the experimental conditions. Comparisons between the certified and the obtained values ranged from 84% (BkF) to 145% (FLT).

The solid material obtained from rainwater (freeze-dried) was hydrolyzed with 1 mL of 2M trifluoroacetic acid (TFA) for 1 h at 100 °C. The samples were dried under vacuum and resuspended in 0.3 mL of deionized water. This was followed by filtration on 0.22 μm (Merck Millipore) filters. The released monosaccharides were analyzed by high-performance anion-exchange chromatography (HPAEC) with pulsed amperometric detection (PAD), with a CarboPac SA10 column (ICS 5.000 system, Dionex-Thermo). The column was eluted isocratically with 99.2% of water and 0.8% (v/v) sodium hydroxide (1 mL min^{-1}). The monosaccharides released from the cell walls were detected using a post-column base containing 500 mM NaOH (0.5 mL min^{-1}) followed by a Pulsed Amperometric Detector. The monosaccharide standards used were apiose, arabinose, fucose, galactose, glucose, mannose, rhamnose, and xylose (Pagliuso et al., 2018).

Turbidity was determined for the rain event samples SA, DI, and EZ, following the protocols described in Baird et al. (2017), with a Lovibond turbidimeter, TurbiCheck SN 13/39540. pH was determined using the multiparameter instrument Lovibond Senso Direct 150.

3. Results and discussions

3.1. Satellite imagery and long-range transport

Satellite imagery from the National Oceanic and Atmospheric Administration's (NOAA) GOES-16 Advanced Baseline Instrument (ABI), and the National Aeronautics and Space Administration's (NASA) Moderate Resolution Imaging Spectroradiometer (MODIS) were recruited to help contextualize the synoptic outlook over the phenomenon area. Fig. 2 shows a large extent of cloud cover over the MASP, registered by both MODIS and ABI between 17:30 to 18:00 UTC (14:30 to 15:00 LT) when the onset of the anomalous sky darkening conditions was observed at the surface. Thick aerosol plumes are shown in Fig. 2 to the west and over the MASP, characterized by a distinct brownish tint over the cloud deck and other cloudless areas. A sequence of enhanced

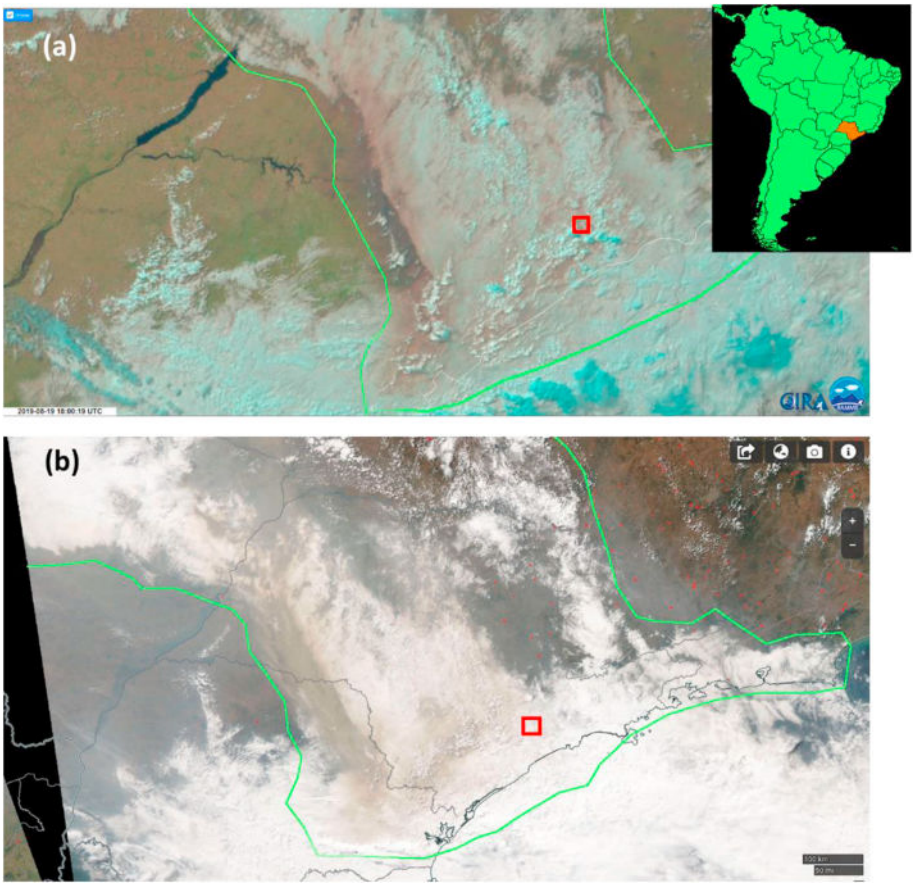

Fig. 2. Satellite imagery over the Metropolitan Area of São Paulo (MASP; square) shows the approximate area covered by a dense smoke-cloud mix (green polygon). (a) Enhanced contrast National Oceanic and Atmospheric Administration's (NOAA) GOES-16 ABI at 2019-08-19 18:00 UTC indicates low-level clouds over the sampling area; (b) National Aeronautics and Space Administration's (NASA) Moderate Resolution Imaging Spectroradiometer (MODIS) onboard Aqua satellite at 17:30 UTC shows fire spots (red dots) and biomass burning smoke plumes covering large extents to the west of São Paulo State in South America (inset).

ABI images, every 10 min from 12:50 to 21:30 UTC (9:50 to 18:30 LT), is given in an external link.[1] The sequence highlights the prevalent easterly to the southeasterly movement of co-located clouds and heavy aerosol-carrying air masses during the event day. An extensive area can be identified west of the MASP where shallow convective clouds simultaneously develop and are transported eastward with the aerosol plumes, eventually forming a clumped cloud deck cluster.[1] The cluster starts to cover the western outskirts of the MASP at about 16:50 UTC (13:50 LT) and proceeds moving over the region past sunset time at 20:51 UTC (17:51 LT).[1] This timing is concurrent with the initiation of the anomalous sky darkening conditions at about 17:30 UTC (14:30 LT), and the precipitation that followed 17:30 UTC to 21:30 UTC (Fig. S3). During this period, Meteorological Aerodrome Reports (METAR) from the three airports in the MASP (SBSP, SBMT, and SBGR) indicate multiple layers of clouds, at about 152.4, 213.4, 914.4, and 3048.0 m above ground level (500, 700, 3,000 and 10,000 ft, AGL).

The origin of the aerosol plumes identified in satellite imagery is discussed next. 3,082 fire spots were detected[2] over the Brazilian Amazon by MODIS onboard the Aqua satellite in the 3-day period between August 17th, and 19th, 2019. During the same period, 1,618 fire spots were detected in Bolivia.[2] On the days preceding the black-rain event, MODIS imagery identified thousands of fire spots and aerosol plumes over Bolivia and the Brazilian Amazon. Smoke from these fire spots was transported downwind, spreading over a large areal fraction of South America. About 24h before the event onset over the MASP MODIS captured a particularly severe burning area[3] over southeastern Bolivia (approximately at −19.1°, −59.6°), where numerous fire spots were detected, which produced vigorous biomass burning smoke plumes moving southeastward.

NOAA's Hysplit model (Rolph et al., 2017) was used to assess the relative contribution of air masses from different origins arriving at the MASP during the event. Ensembles of back (forward) trajectories were calculated starting at 250 m, 1000 m, and 3000 m above ground level (AGL), and on 16Z, 18Z, and 20Z over MASP (Bolivia). Fig. 3 (left) shows one of such ensembles, and the others are shown in Fig. S1. These trajectories are compatible with the convergence of different air masses over the MASP and consistent with meteorological reports. Moist air masses arriving from the ocean were organized by a passing cold front, inducing low-level cloud formation. Air masses arriving over the MASP at mid-level (1–3 km, Fig. S1) traveled from southern Amazon and Bolivia at a range of altitudes, some reaching lower levels in a smoke burdened atmospheric layer close to the surface, then were sharply taken aloft closer to the MASP, rising back to 1000–3000 m AGL over the cloud deck region shown in Fig. 2.

On the right side of Fig. 3 forward trajectories starting about 24h before the MASP event show the path followed by air masses originating over a region in Bolivia[3] heavily impacted by fires and smoke emitted from biomass burning. These trajectories, and those shown in Fig. S2,

[1] GOES-16 ABI sequence (48 MB): https://bit.ly/2019-08-19-SP-GOES16. Accessed May 30th,2020 12:00 UTC.

[2] http://queimadas.dgi.inpe.br/queimadas/bdqueimadas. Accessed May 30th, 2020 13:00 UTC.

[3] https://go.nasa.gov/2TWk6hj and https://go.nasa.gov/3gGdy0d. Accessed May 30th, 2020 14:00 UTC.

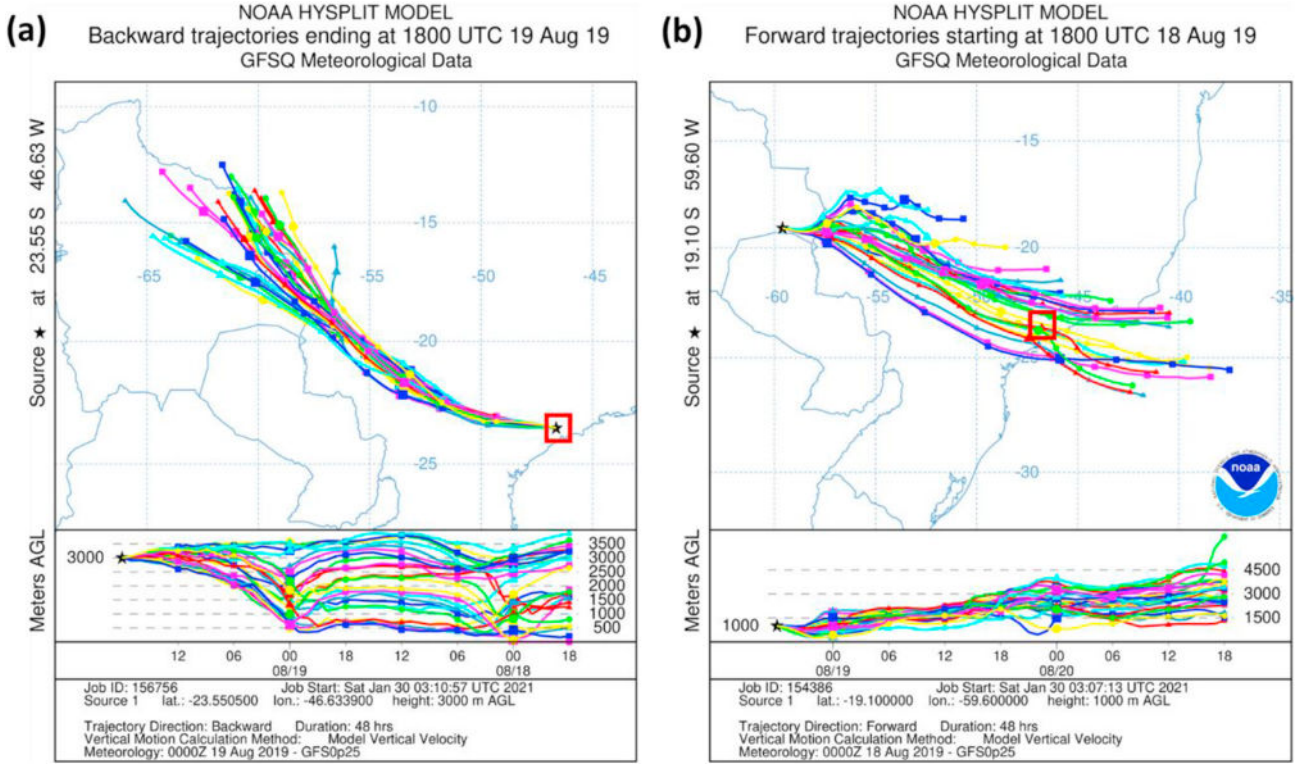

Fig. 3. NOAA's Hysplit model backward and forward trajectories. (a) Back trajectories starting over the MASP indicate the convergence of moist low-level air masses coming from the ocean (east of the MASP), and hotter, drier air masses aloft from the Amazon Basin and Bolivia, bringing smoke aerosol to the MASP. (b) Forward trajectories starting over a Bolivian severe burning area about 24h before the event indicate aerosol plumes were transported toward the MASP. Other starting altitudes and times are shown in Figs. S1 and S2.

indicate that the dense plumes of aerosol emission from this particular area in southeastern Bolivia may have had a significant impact on the MASP event.

3.2. Physical assessment

In the "black rain" samples collected in DI, SA, and EZ, the turbidity was estimated to be above 70 Nephelometric Turbidity Units (NTU). According to the United States Environmental Protection Agency (USEPA) guidelines, non-potable urban water for reuse should not present turbidity equal or higher than 2 NTU for 24 h periods, and not exceed 5 NTU any time (Mendez et al., 2011; USEPA, 2004). The freeze-dried materials in those samples were photographed (Fig. 4) showing that, at least for the water obtained from the collection at the SA and DI sites, some fibrous materials could be visualized, along with particular material with the aspect of burned materials. Such fibers are likely to be part of plant materials such as fiber cells (or cell bundles) of the vascular system of trees and grasses that originated from incomplete combustion that ended up transported and precipitated with the rain. The chemical analyses of these materials, shown below, indicates that plant materials are indeed present and, besides chemical composition evidence (Section 3.4), these materials are the more likely to have maintained reasonably intact chemical structures due to the compactness and probably the hydration level of polymers in the vascular bundles and fibers of wood and leaves.

3.3. Water-soluble ions

The concentrations of water-soluble ions are presented in Table 1. In general, the most abundant cations were K^+ and Ca^{2+} (total average of 165 and 228 μmol L^{-1}, respectively), while the most abundant anions were Cl^- and SO_4^{2-} (total average of 98 and 33 μmol L^{-1}, respectively). The species NH_4^+, NO_2^-, and NO_3^- were not considered since they are observed in household cleaning products and part of the samples came from the household collection (all samples except the ones collected at WZ2). The average concentrations of all ions except Mg^{2+}, formate (CHO_2^-), and acetate ($C_2H_3O_2^-$) were higher in the rainwater samples collected on August 19th, when the "black rain" episode was observed. Organic species, as formate and acetate, are biodegradable (Vet et al., 2014), which may affect their concentration in the samples. Some ionic species as Mg^{2+} can be related to other sources in the site, such as soil dust and urban dust surface resuspension (Rocha et al., 2003). The ionic species concentrations reduced after the event. The measured pH values during the event were 8.2, 7.5, and 7.1 for the EZ, DI, and SA samples, respectively; not acidic.

Species as K^+ and Cl^- can be observed in the particulate matter emitted in the process of biomass burning (Allen et al., 2004; Pereira et al., 2017b), and more soluble particulate matter can act as cloud condensation nuclei and form cloud droplets (Seinfeld, 2004), carrying these species. Potassium maximum monthly concentration has been observed in the dry periods in São Paulo in a previous study that took place between 2002 and 2005, and its presence was partly attributed to biomass burning (Vieira-Filho et al., 2013); in that previous study, sulfate has been observed as a dominant species and related mostly to anthropogenic emission processes in the Metropolitan Area of São Paulo, the average concentrations of potassium and sulfate being of 4.89 and 16.7 μmol L^{-1}, respectively. Potassium concentration in Vieira-Filho et al. (2013) reached a value of 10.9 μmol L^{-1} during excess events, much lower than the values observed in the dark rainwater event (range of 41–402 μmol L^{-1}).

The ratio $[K^+]/[SO_4^{2-}]$ was above or equal to 1.5 in the collected "black rain" samples; this value has been associated by Vieira-Filho et al.

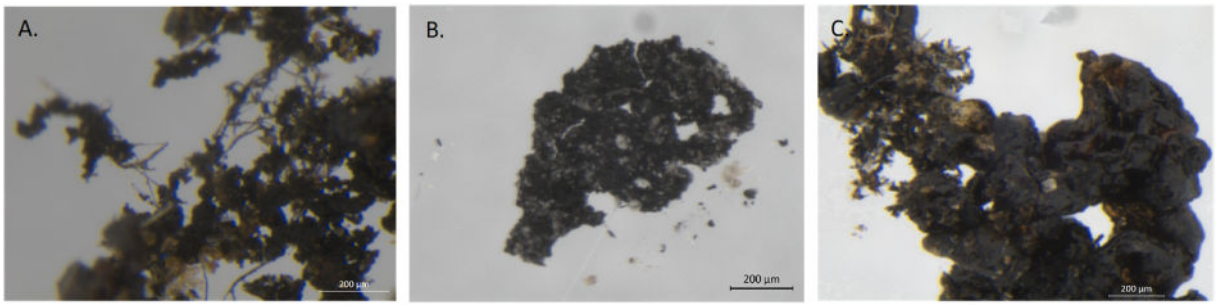

Fig. 4. Freeze-dried solid materials obtained after freeze-drying the rainwater of the "black rain" that occurred on August 19th of 2019 in the Metropolitan Area of São Paulo. The materials are from the following localities: City of Santo André (SA) (a), East Zone of São Paulo City (EZ) (b), City of Diadema (DI) (c).

Table 1
Water-soluble ions concentrations (μmol L^{-1}) and depositions, in parentheses (mg m^{-2}), for all rainwater samples, including periods during and after the "black rain" event. Avg. BR = Average during the "black rain" event. Avg. NR = Average during normal rain events. <LOD = Below limit of detection. <LOQ = Below limit of quantification. Depositions fluxes were considered as zero when concentrations were below the detection and/or quantification limits.

	19Aug EZ	19Aug SZ	19Aug DI	19Aug SA	Avg. BR	01Sep NZ	01Sep WZ1	03Sep WZ2	05Sep WZ2	06Sep WZ2	Avg. NR
Concentration (μmol L^{-1})											
Na^+	33	45	51	84	53	79	64	10	<LOQ	<LOQ	51
K^+	41	193	402	175	203	294	26	<LOD	<LOD	22	114
Ca^{2+}	241	416	338	263	315	492	195	33	36	35	158
Mg^{2+}	30	70	56	57	53	95	28	<LOQ	<LOD	<LOQ	61
Cl^-	25	62	261	75	106	172	83	<LOQ	<LOQ	5	87
SO_4^{2-}	27	65	51	54	49	19	47	8	12	18	21
$C_2O_4^{2-}$	7	12	10	13	10	1	3	<LOD	<LOD	2	2
CHO_2^-	32	<LOD	2	3	12	<LOD	10	26	29	72	34
$C_4H_2O_4^{2-}$	<LOQ	0.5	0.5	0.7	0.6	0.5	<LOD	<LOD	<LOD	<LOD	0.5
$C_4H_4O_4^{-2}$	6	3	22	28	15	11	2	3	1	6	5
$C_5H_6O_4^{2-}$	<LOD	<LOD	1.5	0.8	1.2	<LOD	<LOQ	<LOQ	<LOD	<LOD	<LOD
$C_2H_3O_2^-$	3	8	3	7	6	2	10	20	22	27	16
Deposition (mg m^{-2})											
Na^+	2	5	5	5	4	53	44	2	0	0	20
K^+	4	34	68	19	31	337	30	0	0	3	74
Ca^{2+}	25	75	59	29	47	578	234	12	2	10	167
Mg^{2+}	2	8	6	4	5	67	21	0	0	0	18
Cl^-	2	10	40	7	15	179	88	0	0	2	54
SO_4^{2-}	7	28	21	14	18	53	134	7	1	13	42
$C_2O_4^{2-}$	2	5	4	3	3	3	8	0	0	1	2
CHO_2^-	3.8	0.0	0.4	0.4	1.1	0.0	14.0	11.0	2.0	24.0	9.9
$C_4H_2O_4^{2-}$	0.0	0.3	0.3	0.2	0.2	1.8	0.0	0.0	0.0	0.0	0.4
$C_4H_4O_4^{-2}$	1.8	1.8	11.2	8.7	5.9	38.1	6.0	3.6	0.1	5.1	10.6
$C_5H_6O_4^{2-}$	0.0	0.0	0.9	0.3	0.3	0.0	0.0	0.0	0.0	0.0	0.0
$C_2H_3O_2^-$	0.5	2.3	0.9	1.1	1.2	2.9	18.0	10.9	1.7	11.7	9.0

(2013) to the long-range transport of pollutants in the rainwater. In this study, transport of air masses from the interior of Brazil (including São Paulo state) was observed, leading to higher levels of potassium concentrations; K^+ concentrations were directly proportional to the observed fire spot numbers. Trajectories pointed to transport from the Midwest and North of Brazil that comprises several states in the termed "arc of deforestation", since many fires related to forest burning are registered there, mainly in the drier months (from June to October) (de Oliveira Alves et al., 2011).

Daily deposition flux was calculated with precipitation data derived from different satellites (CHIRPS, CMORPH, and TRMM) and the weather radar; the species concentrations were multiplied by the rainfall amount, similarly as in Roy et al. (2019). Since the precipitation was much lower during the event, most of the ion depositions were higher after the event than during it. The average daily depositions for sulfate and potassium during the "black rain" event were of 18 and 31 mg m^{-2}, respectively, and in the following samples, of 42 and 74 mg m^{-2}, respectively.

Potassium is related to biomass and biogenic processes in wet and dry deposition (Pauliquevis et al., 2012; Vieira-Filho et al., 2013), the species' deposition flux presented a reduction after the event, with lowest values observed in WZ and WZ2, although there was an outlier (NZ) where a very high deposition was observed, 337 mg m^{-2}. Wet deposition of non-sea salt sulfur (which is related to sulfate) is typically higher in southeastern Brazil, and lower in the remote areas of Amazonia (Vet et al., 2014). The observed sulfate in São Paulo rainwater is more associated with secondary reactions of SO_2 emitted by vehicles and has decreased in the previous decades (Fornaro and Gutz, 2006).

If we extrapolate the results presented in this study, the yearly deposition for sulfate and potassium during the "black rain" event would be of 6.4 and 11.4 g m^{-2} yr^{-1}; in a previous study, performed two decades ago, the wet deposition observed in São Paulo for sulfate and potassium were of 2.5 and 0.35 g m^{-2} yr^{-1} (Rocha et al., 2003), it is possible to observe much higher potassium deposition during the event in the present study.

3.4. Plant biomass and biomass burning tracers

The samples collected on August 19th, during the "black rain" event, presented much higher concentrations of levoglucosan than in the other days (Fig. 5), with an average of 0.33 and 0.02 μg mL^{-1}, respectively. The higher levels of these tracers suggest a greater influence of biomass burning aerosols during the event (Mullaugh et al., 2014). The highest levoglucosan concentrations were observed at the cities of Diadema and

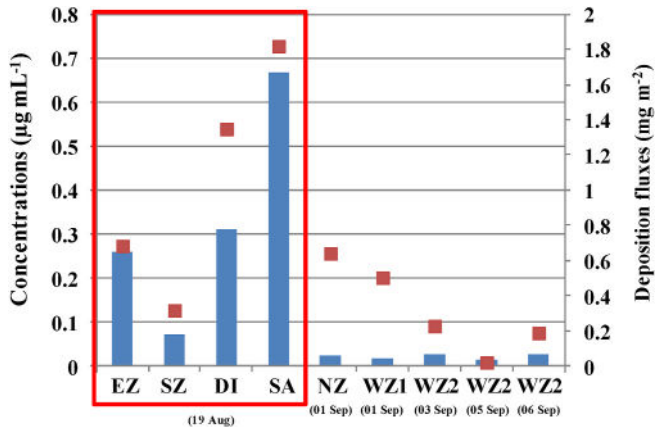

Fig. 5. Levoglucosan concentrations and daily deposition fluxes (blue bars and red squares, respectively) of rainwater samples collected at MASP during the "black rain" event (inside the red rectangular box) and after.

Santo André, both east of the Metropolitan Area of São Paulo, reaching values of 0.31 and 0.67 μg mL^{-1}, respectively. In a previous study performed in the Amazon region (dry period), the levoglucosan concentration reached a higher value of 1.5 μg mL^{-1} (qualitative) (Schkolnik et al., 2005). The presence of the monosaccharide anhydride was attributed to in-cloud processes related to biomass burning aerosols, by mixing of cloud droplets and smoke particles or droplet nucleation on smoke particles, although it also could be attributed to rain scavenging.

The daily average deposition flux for levoglucosan was more than three times higher during the "black rain" event, of 1.04 mg m^{-2} (ranging from 0.32 to 1.82 mg m^{-2}), after the event the average was of 0.31 mg m^{-2} (ranging from 0.02 to 0.64 mg m^{-2}) (Fig. 5). The ratio between the depositions of levoglucosan and SO_4^{2-} was proposed by the authors to understand the influence of biomass burning in the rainwater samples in the present study, since sulfate in São Paulo is more related to a secondary formation from precursor SO_2 emitted by vehicles (Rocha et al., 2003); the ratio was of 0.08 during the event and of 0.02 after it, corroborating to a higher biomass burning influence in the dark rainwater samples.

Mannosan and galactosan were detected in all samples collected during the "black rain" event (average concentrations of 0.07 and 0.05 μg mL^{-1}, respectively), and could not be quantified in most of the post-event rainwater (North Zone, 01 September); it was not possible to associate Lev/Man ratio to sources since it varied between 1.0 and 8.5 in the "black rain" samples).

Cell wall monosaccharides were determined (fucose, arabinose, galactose, rhamnose, glucose, xylose, and mannose) and are presented in Table 2. The combination of monosaccharides found is typical of higher plants (Buckeridge, 2018), indicating that plant materials are present in the particulate matter that precipitated with rainwater during the "black rain". Although the small amount of dry material did not afford the calculation of monosaccharides per mass of particulate matter, Table 2 shows that glucose, probably from cellulose, xylose, and mannose are the most abundant components. Galactose, arabinose, fucose, and rhamnose are also present as less abundant compounds. These results suggest that the major components are cellulose, xylans, and mannans (Schädel et al., 2010; Souza et al., 2013). These polymers are typical components of the wood and plant materials, being present in vascular systems of woods and leaves of trees, including palm trees (mannans) (Carpita and Gibeaut, 1993). The less abundant compounds (arabinose, galactose, fucose, and rhamnose) are also evidence of the presence of plant materials present in the cell walls of plants because they are typical components of pectin polymers (Schädel et al., 2010; Souza et al., 2013). Thus, the observation of fibers in microscopic views (Fig. 4) and the sugar composition of the freeze-dried materials (Table 2) are indicative that the particulate matter brought from the South American hinterland and that precipitated as the "black rain" in São Paulo are a result of partially combusted plant materials.

3.5. Polycyclic aromatic hydrocarbons

The results of the 15 PAHs compounds analyzed in rainwater in MASP are summarized in Fig. 6. The concentrations of total PAHs (∑PAHs) were one hundred times higher for the samples collected during the "black rain" event (EZ = 2155 ng mL^{-1}, SA = 2322 ng mL^{-1}, DI = 1810 ng mL^{-1}, SZ = 194 ng mL^{-1}) than the regular rainy days (WZ1 = 24 ng mL^{-1}, WZ2* = 122 ng mL^{-1}, NZ = 187 ng mL^{-11}); ∑PAHs also presented higher deposition flux during the event (5.1 and 2.7 mg m^{-2}, respectively). Among the PAHs classified as carcinogenic by IARC (2010), benzo[*a*]pyrene (BaP) was detected in high quantities in all samples collected during the event (Fig. 6a, 6b, 6c, and 6d) and in other two samples of the regular days (Fig. 6e, 6f, and 6g). The sample collected at East Zone (EZ, Fig. 6b) showed a predominance of FLT (653 ng mL^{-1}), PHE (433 ng mL^{-1}), and PYR (258 ng mL^{-1}). For the rainwater collected at Santo André city (SA, Fig. 6a), in MASP, the most abundant PAHs were PHE (1467 ng mL^{-1}), BbF (464 ng mL^{-1}), and FLU (67 ng mL^{-1}). Following, another sample collected at MASP, in Diadema city (DI, Fig. 6c), showed a high concentration of PHE (905 ng mL^{-1}), BbF (302 ng mL^{-1}), and FLU (229 ng mL^{-1}). The last sample collected during the "black rain" was from the South Zone of São Paulo City (SZ, Fig. 6d), and its dominant compounds were BbF (44 ng mL^{-1}), FLT (39 ng mL^{-1}), and CHR (23 ng mL^{-1}).

Retene, a marker of biomass burning, was qualitatively identified in all four samples collected during the "black rain" episode (Ramdahl, 1983), by injection of a solution of qualitative retene standard, which allowed searching this compound in the samples. This species has been found as the most abundant PAH in particulate matter during dry season biomass burning episodes in the Amazon region and attributed to DNA damage and cell death *in vitro* (de Oliveira Alves et al, 2011, 2014, 2017). In particulate matter, the predominance of the low molecular weight (LMW) PAHs PHE, FLT, and PYR may indicate an influence of biomass burning emissions (Simoneit, 2002). On average, PHE, FLT, and PYR presented higher deposition fluxes during the event; the fluxes during the event were of 2.3, 0.5, and 0.19 mg m^{-2}, respectively, and after were of 0.4, 0.2 and 0.05 mg m^{-2}. Among the high molecular weight (HMW) PAHs there was a predominance of BbF; this species is cited as a probable human carcinogen and found in particulate matter from vehicular emissions (Pereira et al., 2017b; Ravindra et al., 2008). Particulate organic pollutants as PAHs can be deposited in the soil, vegetation, and waters after wet deposition by precipitation, bringing risks to terrestrial and aquatic life (Malik et al., 2007; Olivella, 2006).

Concerning the rainwater collected in September, the one collected

Table 2
Monosaccharide composition of the particulate matter obtained from the "black rain" in the Metropolitan Area of São Paulo (μg of sugar hydrolyzed per 300 μL of water) on sites at East Zone of São Paulo (EZ), Diadema (DI), and Santo André (SA) (August 19th). The composition was obtained after hydrolysis with trifluoracetic acid followed by High-Performance Anion-Exchange Chromatography (HPAEC) with Pulsed Amperometric Detection (PAD).

(μg sugar per 300 μL of water)	Fucose	Arabinose	Galactose	Rhamnose	Glucose	Xylose	Mannose
EZ	3.5	6.8	12.8	4.4	19.8	10.4	11.5
DI	3.9	13.3	12.7	3.0	47.7	13.6	12.9
SA	9.9	19.2	19.1	10.0	90.9	87.7	35.8

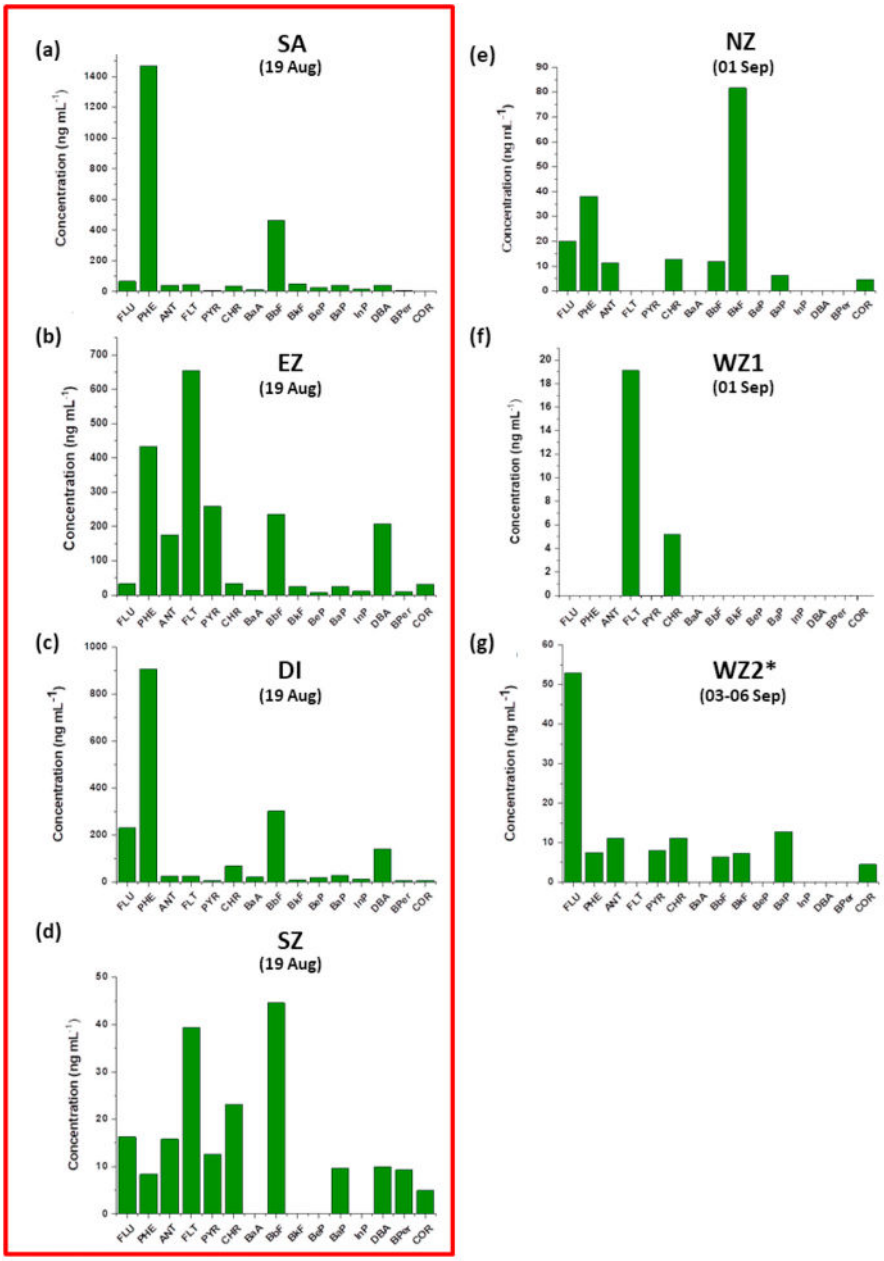

Fig. 6. PAHs concentrations of rainwater samples collected at MASP during the "black rain" event (inside the square) and after. The three samples collected at WZ2* were pooled for this analysis.

at the West Zone of São Paulo City (WZ1, Fig. 6f) presented only two between fifteen PAHs possible to determine, which were FLT (19 ng mL^{-1}), and CHR (5 ng mL^{-1}). In the other samples collected at West Zone (WZ2*, Fig. 6g), nine PAHs were determined, which were FLU (53 ng mL^{-1}), BaP (13 ng mL^{-1}), and CHR (11 ng mL^{-1}), also retene was not found in this sample. Lastly, in the North Zone (NZ, Fig. 6e), the rainwater contained eight in fifteen PAHs, and the dominant species were BkF (82 ng mL^{-1}), PHE (38 ng mL^{-1}), and FLU (20 ng mL^{-1}), this time, the retene was identified.

The tendency of the predominance of some PAHs, such as PHE, PYR, FLT, and FLU, was observed in previous studies conducted with rainwater collected in urban areas (Delhomme et al., 2008; Huybrechts et al., 2016). Although it is difficult to compare values obtained in the present work with other studies since the atypical event occurred in MASP in August, the concentrations were high compared to results obtained during polluted events in France (Delhomme et al., 2008) and India (Malik et al., 2007), the sampling and analytical methods do not allow a direct comparison. In rainwater collected at a subalpine area in Northern Italy, from July 2003 and January 2004, the most abundant compounds were BaA (18.4 x 10^{-3} ng mL^{-1}) and FLT (17.2 x 10^{-3} ng mL^{-1}) (Olivella, 2006), which are one thousand times lower than the present study; another study conducted with rainwater runoff from recovery and recycling companies in Flanders region (Belgium) presented a PHE maximum concentration of 130 ng mL^{-1}, as well as FLT maximum concentration of 88 ng mL^{-1} (Huybrechts et al., 2016), these values were similar to those obtained in this work.

Further, the lower molecular weight (LMW) PAHs dominated over the high molecular weight (HMW) compounds (Fig. 7). In the atmosphere, HMW-PAHs (with four or more aromatic rings), such as benzo [*a*]pyrene, are dominant in the particulate matter (PM) due to their low vapor pressure. In contrast, LMW-PAH (with three or fewer aromatic rings) are more abundant in the gaseous phase, where they react with other pollutants such as ozone and NO_x to form more toxic compounds. Both gaseous and particulate PAHs can be removed by wash-out (below cloud scavenging) and rain out (in-cloud scavenging) (Cousins et al., 1999; Liu et al., 2015; Park et al., 2001; Ravindra et al., 2008), which may have occurred in the contact of the different air masses during that event. For the samples collected during the "black rain" (EZ, SA, DI, and SZ), compounds with three or four rings were more predominant than those with five and six rings, indicating that PAHs in the gaseous phase (three rings) may have been removed by rain-out and wash-out. In the gas phase, SVOC with lower Henry's Law constants, as LMW-PAHs, are more scavenged by precipitation (Cousins et al., 1999). Additionally,

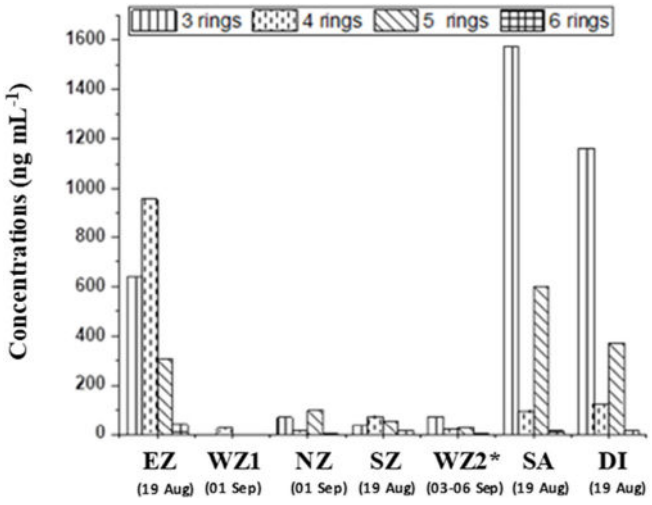

Fig. 7. PAHs concentration for three, four, five, and six rings collected in the "black rain" event and after. The three samples collected at WZ2* were pooled for this analysis.

PAHs with four rings can be found in both particulate and gaseous phases and showed a great contribution. This may occur due to the physical-chemical properties of the compounds. For example, the water solubility is higher for the lower molecular weight PAHs than for the higher molecular weight PAHs (Malik et al., 2007).

The ratio between PAHs can be useful for sources apportionment, for instance, being used to detect combustion-derived aerosols. In general, combustion and/or anthropogenic aerosols are frequently inferred from a rise in the fraction of the less stable PAHs, so the ratio between isomers can support the source identification (Yunker et al., 2002). Table S1 shows the calculated ratios for the present study comparing to the literature values. FLT/(FLT+PYR) ratios, ranged from 0.72 to 0.86 for the rainwater collected in the "black rain" event. Aerosols from urban regions presented values between 0.52 and 0.56, while the value for bush fire particulate matter was of 0.61 (Freeman and Cattell, 1990; Yunker et al., 2002). Darkened rain samples presented a high range of values compared to literature, while for regular rain days it was not possible to calculate this ratio because the concentration of these PAHs had been under the detection limit. This finding probably shows a unique profile concerning forest fires' contributions to wet deposited PAHs. According to previous studies, InP/(InP+BPer) ratios vary less in urban locations than in remote areas. The present work found InP/(InP+BPer) ratios near bush fire particulate matter (0.70) (Freeman and Cattell, 1990; Yunker et al., 2002).

4. Conclusions

An unforeseen darkened rainwater event was observed on August 19th, 2019 throughout the Metropolitan Area of São Paulo, and the collected samples were physically and chemically characterized and compared to control samples from after that event. On that day, winds transported thick plumes of biomass burning aerosols from both Brazilian and the Bolivian Amazon Basins and also in other areas in Bolivia. These air masses converged over the MASP, darkening the early afternoon sunlight when the "black rain" event was registered, as it was observed by a sequence[4] of satellite imagery. These darkened rainwater samples presented high turbidity and fibrous structures were observed together with particulate material with a burned aspect, after freeze-drying; in these freeze-dried particles, glucose (derived from cellulose), xylose, and mannose were the most abundant monosaccharides, corroborating the influence of partially combusted plant materials. Other chemical pieces of evidence of the influence of biomass burning emissions were found, the samples collected during the event presented much higher concentrations of tracers as potassium, levoglucosan, mannosan, and galactosan than the control samples; the deposition flux of organic biomass burning tracers was more than three times higher during the event. It was observed that the "black rain" samples presented increased PAHs concentrations if compared to later rain events, since these species also presented a higher deposition flux during the event. Some of the detected PAHs (retene and benzo[*b*]fluoranthene) have been previously related to adverse health effects; these organic pollutants can contaminate soil, vegetation, and waters after wet deposition by precipitation. The results are of great concern since increased forest fires and deforestation are associated with climate change and the long-range transport of aerosols can affect different countries in the subcontinent (Brazil and Bolivia), leading to public health and environmental impacts.

Data statement

The data is available, if needed it can be provided by the authors.

[4] https://bit.ly/2019-08-19-SP-GOES16. Accessed May 30th, 2020 12: 00UTC.

CRediT authorship contribution statement

Guilherme Martins Pereira: Methodology, Validation, Investigation, Visualization, Writing - original draft. **Sofia Ellen da Silva Caumo:** Methodology, Investigation, Validation, Writing - original draft. **Adriana Grandis:** Methodology, Validation, Investigation, and, Writing - original draft. **Emerson Queiroz Mota do Nascimento:** Investigation. **Alexandre Lima Correia:** Investigation, and, Writing - original draft. **Henrique de Melo Jorge Barbosa:** Investigation, Supervision, Writing - review & editing, and, Writing - original draft, Review and Editing. **Marta Angela Marcondes:** Investigation, Funding acquisition, Writing - original draft. **Marcos Silveira Buckeridge:** Supervision, Funding acquisition, Writing - review & editing. **Pérola de Castro Vasconcellos:** Conceptualization, Supervision, Project administration, Funding acquisition, and, Writing - review & editing.

Declaration of competing interest

The authors declare that they have no known competing financial interests or personal relationships that could have appeared to influence the work reported in this paper.

Acknowledgments

The authors gratefully acknowledge the NOAA Air Resources Laboratory (ARL) for the provision of the HYSPLIT transport and dispersion model and READY website (https://www.ready.noaa.gov) used in this publication. The authors thank FAPESP (2010/15959-3, 2016/23339-1, 2016/18866-2, 2018/16608-1, 2019/01316-8, and 2019/13936-0), São Paulo Research Foundation, and CNPq (308682/20173, 301503/2018-4, 429112/2018-1, and 120779/2019-6), National Council for Scientific and Technological Development. This work was also supported by the National Institute of Science and Technology of Bioethanol (INCT-Bioethanol) (FAPESP 2008/57908-6 and 2014/50884-5; CNPq 574002/2008-1 and 465319/2014-9). The authors thank Professor Theotonio Mendes Pauliquevis Júnior for reviewing and suggesting important improvements to this paper.

Appendix A. Supplementary data

Supplementary data to this article can be found online at https://doi.org/10.1016/j.atmosenv.2021.118229.

References

Allen, A.G., Cardoso, A.A., da Rocha, G.O., 2004. Influence of sugar cane burning on aerosol soluble ion composition in Southeastern Brazil. Atmos. Environ. 38, 5025–5038. https://doi.org/10.1016/j.atmosenv.2004.06.019.

Altieri, K.E., Seitzinger, S.P., Carlton, A.G., Turpin, B.J., Klein, G.C., Marshall, A.G., 2008. Oligomers formed through in-cloud methylglyoxal reactions: chemical composition, properties, and mechanisms investigated by ultra-high resolution FT-ICR mass spectrometry. Atmos. Environ. 42, 1476–1490. https://doi.org/10.1016/j.atmosenv.2007.11.015.

Andrade, M. de F., Kumar, P., de Freitas, E.D., Ynoue, R.Y., Martins, J., Martins, L.D., Nogueira, T., Perez-Martinez, P., de Miranda, R.M., Albuquerque, T., Gonçalves, F.L. T., Oyama, B., Zhang, Y., 2017. Air quality in the megacity of São Paulo: evolution over the last 30 years and future perspectives. Atmos. Environ. 159, 66–82. https://doi.org/10.1016/j.atmosenv.2017.03.051.

Andreae, M.O., Rossenfeld, D., Artaxo, P., Costa, A.A., Frank, G.P., Longo, K.M., Silva-Dias, M.A., 2004. Smoking rain clouds over the Amazon. Science 303, 1337–1343. https://doi.org/10.1126/science.1092779.

Artaxo, P., Rizzo, L.V., Brito, J.F., Barbosa, H.M.J., Arana, A., Sena, E.T., Cirino, G.G., Bastos, W., Martin, S.T., Andreae, M.O., 2013. Atmospheric aerosols in Amazonia and land use change: from natural biogenic to biomass burning conditions. Faraday Discuss 165, 203–235. https://doi.org/10.1039/c3fd00052d.

Avery, G.B., Kieber, R.J., Witt, M., Willey, J.D., 2006. Rainwater monocarboxylic and dicarboxylic acid concentrations in southeastern North Carolina, USA, as a function of air-mass back-trajectory. Atmos. Environ. 40, 1683–1693. https://doi.org/10.1016/j.atmosenv.2005.10.058.

Baird, R.B., Eaton, A.D., Rice, E.W., 2017. Standard Methods for the Examination of Water and Wastewater, 23rd ed.

Buckeridge, M.S., 2018. The evolution of the Glycomic Codes of extracellular matrices. Biosystems 164, 112–120. https://doi.org/10.1016/j.biosystems.2017.10.003.

Carpita, N.C., Gibeaut, D.M., 1993. Structural models of primary cell walls in flowering plants: consistency of molecular structure with the physical properties of the walls during growth. Plant J. 3, 1–30. https://doi.org/10.1111/j.1365-313X.1993.tb00007.x.

Cousins, I.T., Beck, A.J., Jones, K.C., 1999. A review of the processes involved in the exchange of semi-volatile organic compounds (SVOC) across the air–soil interface. Sci. Total Environ. 228, 5–24. https://doi.org/10.1016/S0048-9697(99)00015-7.

Darbyshire, E., Morgan, W.T., Allan, J.D., Liu, D., Flynn, M.J., Dorsey, J.R., O'Shea, S.J., Lowe, D., Szpek, K., Marenco, F., Johnson, B.T., Bauguitte, S., Haywood, J.M., Brito, J.F., Artaxo, P., Longo, K.M., Coe, H., 2019. The vertical distribution of biomass burning pollution over tropical South America from aircraft in situ measurements during SAMBBA. Atmos. Chem. Phys. 19, 5771–5790. https://doi.org/10.5194/acp-19-5771-2019.

de Almeida Silva, M., Almeida de Holanda, L., Pereira Sartori, M.M., Germino, G.H., de Moraes Barbosa, A., Bianchi, L., 2020. Base cut quality and productivity of mechanically harvested sugarcane. Sugar Technol. 22, 284–290. https://doi.org/10.1007/s12355-019-00768-z.

de Oliveira Alves, N., Brito, J., Caumo, S., Arana, A., Hacon, S. de S., Artaxo, P., Hillamo, R., Teinilä, K., de Medeiros, S.R.B., Vasconcellos, P. de C., 2015. Biomass burning in the Amazon region: aerosol source apportionment and associated health risk assessment. Atmos. Environ. 120, 277–285. https://doi.org/10.1016/j.atmosenv.2015.08.059.

de Oliveira Alves, N., Hacon, S. de S., Galvão, M.F. de O., Peixoto, M.S., Artaxo, P., Vasconcellos, P. de C., de Medeiros, S.R.B., 2014. Genetic damage of organic matter in the Brazilian Amazon: a comparative study between intense and moderate biomass burning. Environ. Res. 130, 51–58. https://doi.org/10.1016/j.envres.2013.12.011.

de Oliveira Alves, N., Matos Loureiro, A.L., dos Santos, F.C., Nascimento, K.H., Dallacort, R., de Castro Vasconcellos, P., de Souza Hacon, S., Artaxo, P., de Medeiros, S.R.B., 2011. Genotoxicity and composition of particulate matter from biomass burning in the eastern Brazilian Amazon region. Ecotoxicol. Environ. Saf. 74, 1427–1433. https://doi.org/10.1016/j.ecoenv.2011.04.007.

de Oliveira Alves, N., Vessoni, A.T., Quinet, A., Fortunato, R.S., Kajitani, G.S., Peixoto, M. S., De Souza Hacon, S., Artaxo, P., Saldiva, P., Menck, C.F.M., De Medeiros, S.R.B., 2017. Biomass burning in the Amazon region causes DNA damage and cell death in human lung cells. Sci. Rep. 7, 1–13. https://doi.org/10.1038/s41598-017-11024-3.

de Oliveira Galvão, M.F., de Oliveira Alves, N., Ferreira, P.A., Caumo, S., de Castro Vasconcellos, P., Artaxo, P., de Souza Hacon, S., Roubicek, D.A., Batistuzzo de Medeiros, S.R., 2018. Biomass burning particles in the Brazilian Amazon region: mutagenic effects of nitro and oxy-PAHs and assessment of health risks. Environ. Pollut. 233, 960–970. https://doi.org/10.1016/j.envpol.2017.09.068.

Delhomme, O., Rieb, E., Millet, M., 2008. Polycyclic aromatic hydrocarbons analyzed in rainwater collected on two sites in east of France (Strasbourg and Erstein). Polycycl. Aromat. Comp. 28, 472–485. https://doi.org/10.1080/10406630802377898.

Duncan, B.N., Martin, R.V., Staudt, A.C., Yevich, R., Logan, J.A., 2003. Interannual and seasonal variability of biomass burning emissions constrained by satellite observations. J. Geophys. Res. Atmos. 108 https://doi.org/10.1029/2002jd002378.

Edwards, D.P., Emmons, L.K., Gille, J.C., Chu, A., Attié, J.L., Giglio, L., Wood, S.W., Haywood, J., Deeter, M.N., Massie, S.T., Ziskin, D.C., Drummond, J.R., 2006. Satellite-observed pollution from Southern Hemisphere biomass burning. J. Geophys. Res. Atmos. 111, 1–17. https://doi.org/10.1029/2005JD006655.

EMS Parameter, 2017. Polycyclic Aromatic Hydrocarbons in Water by GC/MS - PBM.

Fornaro, A., Gutz, I.G.R., 2006. Wet deposition and related atmospheric chemistry in the São Paulo metropolis, Brazil. Part 3: trends in precipitation chemistry during 1983-2003. Atmos. Environ. 40, 5893–5901. https://doi.org/10.1016/j.atmosenv.2005.12.007.

Freeman, D.J., Cattell, F.C.R., 1990. Woodburning as a source of atmospheric polycyclic aromatic hydrocarbons. Environ. Sci. Technol. 24, 1581–1585. https://doi.org/10.1021/es00080a019.

Fu, P., Kawamura, K., Kobayashi, M., Simoneit, B.R.T., 2012. Seasonal variations of sugars in atmospheric particulate matter from Gosan , Jeju Island : significant contributions of airborne pollen and Asian dust in spring. Atmos. Environ. 55, 234–239. https://doi.org/10.1016/j.atmosenv.2012.02.061.

Huybrechts, D., Verachtert, E., Vander Aa, S., Polders, C., Van den Abeele, L., 2016. Polluted rainwater runoff from waste recovery and recycling companies: determination of emission levels associated with the best available techniques. Waste Manag. 54, 74–82. https://doi.org/10.1016/j.wasman.2016.05.002.

IARC, 2010. IARC Monographs on the Evaluation of Carcinogenic Risks to Humans.

Koren, I., Kaufman, Y.J., Remer, L.A., Martins, J.V., 2004. Measurement of the effect of Amazon smoke on inhibition of cloud formation. Science 303, 1342–1346. https://doi.org/10.1126/science.1089424.

Liu, Y., Gao, Y., Zhang, C., Wang, S., Ma, L., Zhao, J., Lohmann, R., 2015. Particulate matter, gaseous and particulate polycyclic aromatic hydrocarbons (PAHs) in an urban traffic tunnel of China: emission from on-road vehicles and gas-particle partitioning. Chemosphere 134, 52–59. https://doi.org/10.1016/j.chemosphere.2015.03.065.

Malhi, Y., Roberts, J.T., Betts, R.A., Killeen, T.J., Li, W., Nobre, C.A., 2008. Climate change, deforestation, and the fate of the Amazon. Science 319, 169–173. https://doi.org/10.1126/science.1146961.

Malik, A., Singh, V.K., Singh, K.P., 2007. Occurrence and distribution of persistent trace organics in rainwater in an urban region (India). Bull. Environ. Contam. Toxicol. 79, 639–645. https://doi.org/10.1007/s00128-007-9290-8.

Mead, R.N., Mullaugh, K.M., Avery, G.B., Kieber, R.J., Willey, J.D., Podgorski, D.C., 2013. Insights into dissolved organic matter complexity in rainwater from

continental and coastal storms by ultrahigh resolution Fourier transform ion cyclotron resonance mass spectrometry. Atmos. Chem. Phys. 13, 4829–4838. https://doi.org/10.5194/acp-13-4829-2013.

Mendez, C.B., Klenzendorf, J.B., Afshar, B.R., Simmons, M.T., Barrett, M.E., Kinney, K.A., Kirisits, M.J., 2011. The effect of roofing material on the quality of harvested rainwater. Water Res. 45, 2049–2059. https://doi.org/10.1016/j.watres.2010.12.015.

Mullaugh, K.M., Byrd, J.N., Jr, G.B.A., Mead, R.N., Willey, J.D., Kieber, R.J., 2014. Characterization of carbohydrates in rainwater from the Southeastern North Carolina. Chemosphere 107, 51–57. https://doi.org/10.1016/j.chemosphere.2014.03.014.

Olivella, M.À., 2006. Polycyclic aromatic hydrocarbons in rainwater and surface waters of Lake Maggiore, a subalpine lake in Northern Italy. Chemosphere 63, 116–131. https://doi.org/10.1016/j.chemosphere.2005.07.045.

Pagliuso, D., Grandis, A., Igarashi, E.S., Lam, E., Buckeridge, M.S., 2018. Correlation of apiose levels and growth rates in duckweeds. Front. Chem. 6, 1–10. https://doi.org/10.3389/fchem.2018.00291.

Park, J.-S., Wade, T.L., Sweet, S., 2001. Atmospheric distribution of polycyclic aromatic hydrocarbons and deposition to Galveston Bay, Texas, USA. Atmos. Environ. 35, 3241–3249. https://doi.org/10.1016/S1352-2310(01)00080-2.

Pashynska, V., Vermeylen, R., Vas, G., Maenhaut, W., Claeys, M., 2002. Development of a gas chromatographic/ion trap mass spectrometric metod for the determination of levoglucosan and saccharidic compounds in atmospheric aerosols. Application to urban aerosols. J. Mass Spectrom. 37, 1249–1257. https://doi.org/10.1002/jms.391.

Pauliquevis, T., Lara, L.L., Antunes, M.L., Artaxo, P., 2012. Aerosol and precipitation chemistry measurements in a remote site in Central Amazonia: the role of biogenic contribution. Atmos. Chem. Phys. 12, 4987–5015. https://doi.org/10.5194/acp-12-4987-2012.

Pereira, G.M., Alves, N.O., Caumo, S.E.S., Soares, S., Teinilä, K., Custódio, D., Hillamo, R., Alves, C., Vasconcellos, P.C., 2017a. Chemical composition of aerosol in São Paulo, Brazil: influence of the transport of pollutants. Air Qual. Atmos. Health 10, 457–468. https://doi.org/10.1007/s11869-016-0437-9.

Pereira, G.M., Oraggio, B., Teinilä, K., Custódio, D., Huang, X., Hillamo, R., Alves, C.A., Balasubramanian, R., Rojas, N.Y., Sanchez-Ccoyllo, O.R., Vasconcellos, P. de C., 2019. A comparative chemical study of PM 10 in three Latin American cities: Lima, Medellín, and São Paulo. Air Qual. Atmos. Health. https://doi.org/10.1007/s11869-019-00735-3.

Pereira, G.M., Teinilä, K., Custódio, D., Santos, A.G., Xian, H., Hillamo, R., Alves, C.A., Andrade, J.B. de, da Rocha, G.O., Kumar, P., Balasubramanian, R., Andrade, M. de F., Vasconcellos, P.C., 2017b. Particulate pollutants in the Brazilian city of São Paulo: 1-year investigation for the chemical composition and source apportionment. Atmos. Chem. Phys. 17, 11943–11969. https://doi.org/10.5194/acp-17-11943-2017.

Ramdahl, T., 1983. Retene—a molecular marker of wood combustion in ambient air. Nature 306, 580–582. https://doi.org/10.1038/306580a0.

Ravindra, K., Sokhi, R., Van Grieken, R., 2008. Atmospheric polycyclic aromatic hydrocarbons: source attribution, emission factors and regulation. Atmos. Environ. 42, 2895–2921. https://doi.org/10.1016/j.atmosenv.2007.12.010.

Rocha, F.R., Fracassi da Silva, J.A., Lago, C.L., Fornaro, A., Gutz, I.G.R., 2003. Wet deposition and related atmospheric chemistry in the São Paulo metropolis, Brazil: Part 1. Major inorganic ions in rainwater as evaluated by capillary electrophoresis with contactless conductivity detection. Atmos. Environ. 37, 105–115. https://doi.org/10.1016/S1352-2310(02)00722-7.

Rolph, G., Stein, A., Stunder, B., 2017. Real-time environmental applications and display sYstem: READY. Environ. Model. Software 95, 210–228. https://doi.org/10.1016/j.envsoft.2017.06.025.

Roy, A., Chatterjee, A., Ghosh, A., Das, S.K., Ghosh, S.K., Raha, S., 2019. Below-cloud scavenging of size-segregated aerosols and its effect on rainwater acidity and nutrient deposition: a long-term (2009–2018) and real-time observation over eastern Himalaya. Sci. Total Environ. 674, 223–233. https://doi.org/10.1016/j.scitotenv.2019.04.165.

Russell, L.M., Hawkins, L.N., Frossard, A.A., Quinn, P.K., Bates, T.S., 2009. Carbohydrate-like composition of submicron atmospheric particles and their production from ocean bubble bursting. Proc. Natl. Acad. Sci. Unit. States Am. 107, 6652–6657. https://doi.org/10.1073/pnas.0908905107.

Santos, A.C.A., 2014. Caracterização de aerossóis no pantanal mato-grossense.

Schädel, C., Blöchl, A., Richter, A., Hoch, G., 2010. Quantification and monosaccharide composition of hemicelluloses from different plant functional types. Plant Physiol. Biochem. 48, 1–8. https://doi.org/10.1016/j.plaphy.2009.09.008.

Schkolnik, G., Falkovich, A.H., Rudich, Y., Maenhaut, W., Artaxo, P., 2005. A new method for the determination of levoglucosan, methyl-erythritol and related compounds and its application for rainwater and smoke samples. Environ. Sci. Technol. 39, 2744–2752. https://doi.org/10.1021/es048363c.

Seinfeld, J.H., 2004. Air pollution: a half century of progress. AIChE J. 50, 1096–1108. https://doi.org/10.1002/aic.10102.

Seinfeld, J.H., Pandis, S.N., 2006. Atmospheric Chemistry and Physics: from Air Pollution to Climate Change, second ed. John Wiley & Sons, New York. 2006.

Sena, E.T., Artaxo, P., Correia, A.L., 2013. Spatial variability of the direct radiative forcing of biomass burning aerosols and the effects of land use change in Amazonia. Atmos. Chem. Phys. 13, 1261–1275. https://doi.org/10.5194/acp-13-1261-2013.

Simoneit, B.R.T., 2002. Biomass burning — a review of organic tracers for smoke from incomplete combustion. Appl. Geochem. 17, 129–162. https://doi.org/10.1016/S0883-2927(01)00061-0.

Simoneit, B.R.T., Kobayashi, M., Kawamura, K., Rushdi, A.I., Rogge, W.F., Didyk, B.M., 2004. Sugars - dominant water-soluble organic compounds in soils and characterization as tracers in atmospheric particulate matter. Environ. Sci. Technol. 38, 5939–5949. https://doi.org/10.1021/es0403099.

Souza, A.P. de, Leite, D.C.C., Pattathil, S., Hahn, M.G., Buckeridge, M.S., 2013. Composition and structure of sugarcane cell wall polysaccharides: implications for second-generation Bioethanol production. BioEnergy Res. 6, 564–579. https://doi.org/10.1007/s12155-012-9268-1.

USEPA, 2004. Guidelines for Water Reuse.

Vasconcellos, P.C., Souza, D.Z., Avila, S.G., Araujo, M.P., Naoto, E., Nascimento, K.H., Cavalcante, F.S., Dos Santos, M., Smichowski, P., Behrentz, E., 2011. Comparative study of the atmospheric chemical composition of three South American cities. Atmos. Environ. 45, 5770–5777. https://doi.org/10.1016/j.atmosenv.2011.07.018.

Vasconcellos, P.C., Souza, D.Z., Sanchez-Ccoyllo, O., Bustillos, J.O.V., Lee, H., Santos, F. C., Nascimento, K.H., Araújo, M.P., Saarnio, K., Teinilä, K., Hillamo, R., 2010. Determination of anthropogenic and biogenic compounds on atmospheric aerosol collected in urban, biomass burning and forest areas in São Paulo, Brazil. Sci. Total Environ. 408, 5836–5844. https://doi.org/10.1016/j.scitotenv.2010.08.012.

Vet, R., Artz, R.S., Carou, S., Shaw, M., Ro, C.U., Aas, W., Baker, A., Bowersox, V.C., Dentener, F., Galy-Lacaux, C., Hou, A., Pienaar, J.J., Gillett, R., Forti, M.C., Gromov, S., Hara, H., Khodzher, T., Mahowald, N.M., Nickovic, S., Rao, P.S.P., Reid, N.W., 2014. A global assessment of precipitation chemistry and deposition of sulfur, nitrogen, sea salt, base cations, organic acids, acidity and pH, and phosphorus. Atmos. Environ. 93, 3–100. https://doi.org/10.1016/j.atmosenv.2013.10.060.

Vieira-Filho, M.S., Pedrotti, J.J., Fornaro, A., 2013. Contribution of long and mid-range transport on the sodium and potassium concentrations in rainwater samples, São Paulo megacity, Brazil. Atmos. Environ. 79, 299–307. https://doi.org/10.1016/j.atmosenv.2013.05.047.

Yunker, M.B., Macdonald, R.W., Vingarzan, R., Mitchell, H., Goyette, D., Sylvestre, S., 2002. PAHs in the Fraser River basin: a critical appraisal of PAH ratios as indicators of PAH source and composition. Org. Geochem. 33, 489–515. https://doi.org/10.1016/S0146-6380(02)00002-5.

Zhu, J., Xia, X., Che, H., Wang, J., Zhang, J., Duan, Y., 2016. Study of aerosol optical properties at Kunming in southwest China and long-range transport of biomass burning aerosols from North Burma. Atmos. Res. 169, 237–247. https://doi.org/10.1016/j.atmosres.2015.10.012.